A New Structure of 12Slot-10Pole Field-Excitation Flux Switching Synchronous Machine for Hybrid Electric Vehicles

Erwan Sulaiman, Takashi Kosaka, Nobuyuki Matsui
Dept. of Electrical & Computer Engineering, Nagoya Institute of Technology,
Gokiso, Showa, Nagoya, Aichi, 466-8555 Japan
Tel.: +81 / (52) – 7355420
Fax: +81 / (52) – 7355420
E-Mail: erwan@motion.elcom.nitech.ac.jp
URL: http://motion.elcom.nitech.ac.jp/

Keywords

«Field-excitation», «Flux switching synchronous machine», «Hybrid electric vehicles», «Finite element analysis»

Abstract

This paper presents a new structure of 12Slot-10Pole field-excitation flux switching synchronous machine (FEFSSM) with all active parts namely field excitation coil (FEC) and armature coil are located on the stator, applied for hybrid electric vehicles (HEVs). The rotor part consists of single piece iron makes it more robust and becoming more suitable to apply for high speed motor drive system application coupled with reduction gear. The design target is the motor with a maximum torque of 210Nm with reduction gear ratio of 4:1, a maximum power of 123kW, a maximum power density more than 3.5kW/kg, and a maximum speed of 20,000r/min with similar restrictions and specifications in IPMSM used for LEXUS RX400h. The deterministic design optimization approach is used to treat design parameters defined in rotor, armature and FEC repeatedly until the target performances are achieved, under maximum current density 21A/mm^2 for both armature and FEC. A result shows that the proposed design enables to keep the same power density in existing IPMSM installed on a commercial SUV-HEV.

Introduction

For more than 100 years, vehicles equipped with conventional internal combustion engine (ICE) have been used for personal transportation. Along with that, with increasing rates of rapid world population, demand for private vehicles is also increasing every day. One of the serious problems associated with ever-increasing use of personal vehicles is the emissions. The green house effect, also known as global warming, is an acute issue that all people have to face. Government agencies and organizations have developed more stringent standards for the fuel consumption and emissions. Nevertheless, with the ICE technology being matured over the past 100 years, although it will continue to improve with the aid of automotive electronic technology, it will mainly rely on alternative evolution approaches to significantly improve the fuel economy and reduce emissions. Therefore, in order to obtain a wide-range full-performance high efficiency vehicle while reducing pollutant emissions, the most feasible solution at present is the hybrid electrical vehicles (HEVs) which combine battery-based electric machines with an ICE [1-4].

Among different types of electric machines, there are four major types that are viable for HEVs, namely, direct current (dc) machines, induction machines, switch reluctance (SR) machines, and permanent magnet brushless (PM BL) machines. DC machines are used to be widely accepted for EVs and HEVs because of their advantage of simple control of the orthogonal disposition of field and armature mmf. Moreover, by replacing the field winding with PMs, the PM dc machines permit a considerable reduction in stator diameter due to the efficient use of radial space. Owing to the low permeability of PMs, armature reaction is usually reduced, and commutation is improved. However,

the principle problem of dc drives, due to their commutators and brushes, makes them less reliable and unsuitable for a maintenance-free operation.

In other circumstances, induction machines are a widely accepted brushless drive for HEVs because of their low cost, high reliability, and freedom from maintenance. However, conventional control of induction drives, such as variable voltage variable frequency, cannot provide the desired performance. The major reason is due to the nonlinearities of their dynamic model. With the advent of microcomputer era, the principle of field-oriented control or vector control of induction drives has been accepted to overcome their nonlinearities. Moreover, the development of EV and HEV induction machines is continually fueled by new design approaches and advanced control strategies [5].

Meanwhile, SR machines have been recognized to have a considerable potential for HEVs. They have the definite advantages of simple construction, low manufacturing cost, and outstanding torque-speed characteristics. Although they possess simplicity in construction, their design and control are difficult and subtle. In addition, they usually exhibit acoustic-noise problems [6-8]. On the other hand, PM BL machines are becoming more and more attractive and can directly compete with the induction machines for HEVs. The definite advantages of PM BL machines are their inherently high efficiency, high power density, and high reliability. The key problem is their relatively high cost due to PM materials. In general, according to the operating current and no-load electromotive-force (EMF) waveforms, they are classified as PM BL ac (BLAC) and PM BL dc (BLDC) types. In recent years, the class of PM BL drives has been expanded to embrace those with hybrid field excitations [9].

One example of successfully developed electric machines for HEVs is interior permanent magnet synchronous machines (IPMSMs) which have been employed mainly to increase the power density of the machines [10-11]. This can be proved by the historical progress in the power density of main traction motor installed on Toyota HEVs. The power density of each motor employed in Lexus RX400h'05 and GS450h'06 have been improved approximately five times and more, respectively, compared to that installed on Prius'97 [12]. Although the torque density of each motor has been hardly changed, a reduction gear has enabled to elevate the axle torque necessary for propelling the large vehicles such as RX400h and GS450h. As one of effective strategies for increasing the motor power density, the technological tendency to employ the combination of a high-speed machine and a reduction gear would be accelerated.

In other circumstances, an increase in annual usage of rare-earth magnet have increased the price of rare-earth metals not only Neodymium (N_d) but also Dysprosium (D_y) and Terbium (T_b) which are indispensable to provide the rare-earth magnet with high coercivity as the additives. According to the report released by Mineral Resource Information Center affiliated to Japan Oil, Gas and Metals National Corporation, a future prospect was summarized such that the production amount of $N_{d2}F_{e14}B$ would reach at 1,500 tons only in HEV applications in 2011 and the corresponding usage of 70 tons Dysprosium would be serious problem from the viewpoints of cost, security and undersupply. Therefore, the continuous research and development of permanent magnet machines with less or no rare-earth materials would be very important [13-15].

As one alternative solution with high possibility to overcome this problem, a new design of 12Slot-10Pole field-excitation flux switching synchronous machine (FEFSSM) with no permanent magnet is proposed. The initial design of this machine is shown in Fig. 1. Both FEC and armature coils are allocated at stator side. The rotor consists of only single piece iron, becoming more robust and more suitable for high speed operation. Although less pole number reduces the supply frequency of inverter, the 12Slot-10Pole machine is selected and proposed in this research because; (1) it can be considered as the best minimum combination of slot-pole to avoid odd rotor pole numbers such as 6Slot-5Pole and 6Slot-7Pole machines yielding unbalanced pulling force, (2) to avoid high torque ripples in case of 6Slot-8Pole and 6Slot-4Pole machines, and (3) to take good balance between rotor and stator pole widths for minimizing inescapable torque pulsation.

FEFSSM operating principle

The term flux switching is coined to describe machines in which the stator tooth flux switches polarity following the motion of a salient pole rotor. All excitation sources are located on the stator with the armature coils and FECs allocated to alternate stator teeth. The FECs produce six north poles interspersed between six south poles. The 12 slots armature coils consists of three phase supply located in each 1/4 stator body and is divided periodically. As the rotor rotates, the segments switch the armature flux so that it alternates up and down in these 12 slots. Each time the rotor rotates through 1/10 of a revolution, the flux linking the armature coils goes through a complete cycle, and so the frequency of the AC emf induced in the stator is ten times the rotational frequency.

The advantages of this machine are easy cooling of all active parts in the stator and robust rotor structure that makes it better suitability for high-speed application compared to conventional IPMSM. On the other hand, the field excitation can be used to control flux with variable flux capabilities. Fig. 2 illustrates the direction of flux linkage caused by mmf of FEC in this machine. This type of machine is classified into flux switching synchronous machines (FSSM) which is also getting more popular and popular in recent years [16-19].

This paper presents an investigation into design possibility of 12Slot-10Pole FEFSSM for traction drives in HEVs. Some design refinements based on 2D-FEA are conducted to achieve better torque-speed characteristics and power production. The design restrictions and specifications for the target HEV applications are discussed in the following section. Subsequently, based on finite element analysis (FEA), the method of getting the maximum performances is explained. Then, the flux line of field excitation at open-circuit condition, the rotor mechanical strength, the torque and power factor versus field excitation current density characteristics, the torque and power versus speed characteristics, the loss and the efficiency are also predicted and discussed. Some conclusions are drawn in the final section.

Design restriction and specifications for HEV applications

The design restrictions and target specifications of the proposed machine for HEV applications are listed in Table I. The table includes the available and estimated specifications of the FEFSSM for same items with IPMSM for LEXUS RX400h as in Ref [11]. The electrical restrictions related with the inverter are set to be much severe. Assuming that only a water cooling system is employed as the

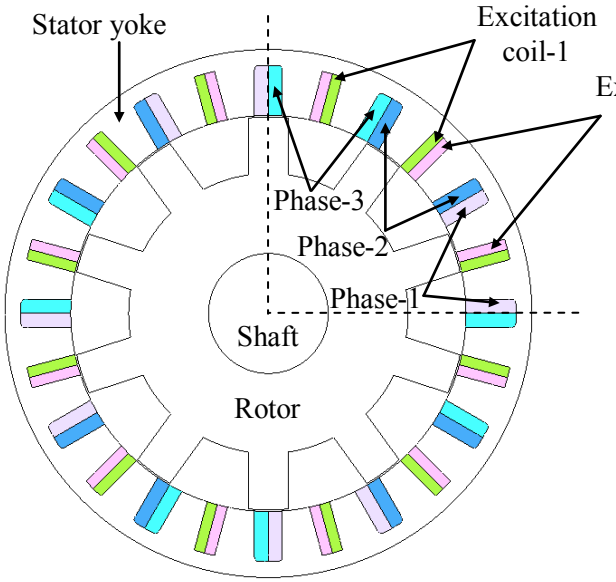

Fig. 1: Initial design of 12Slot-10Pole FEFSSM

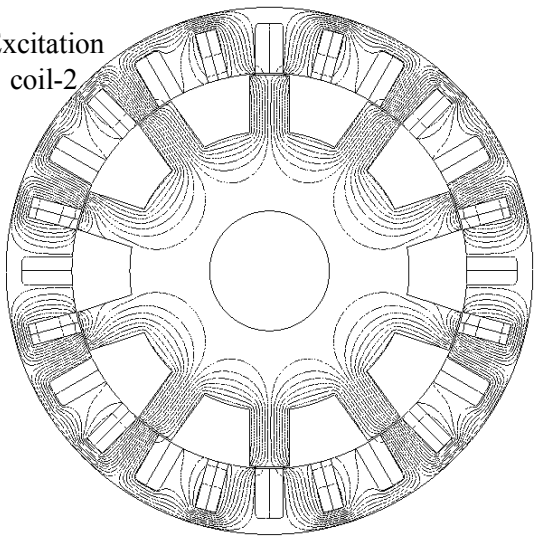

Fig. 2: Flux paths caused by mmf of field-excitation in 12Slot-10Pole FEFSSM

Table I: FEFSSM design restrictions and specifications for HEV applications

Items	IPMSM RX400h	FEFSSM
Max. DC-bus voltage inverter (V)	650	650
Max. inverter current (A_{rms})	Conf.	250
Max. current density in armature winding, J_a (A_{rms}/mm^2)	Conf.	21
Max. current density in excitation winding, J_e (A/mm^2)	NA	21
Stator outer diameter (mm)	264	264
Motor stack length (mm)	70	70
Shaft radius (mm)	30	30
Air gap length (mm)	0.8	0.8
Permanent magnet weight (kg)	1.1	0.0
Maximum speed (r/min)	12,400	20,000
Maximum torque (Nm)	333	> 210
Reduction gear ratio	2.478	4
Max. axle torque via reduction gear (Nm)	825	> 840
Max. power (kW)	123	> 123
Power density (kW/kg)	3.5	> 3.5

cooling system of the machine, the limit of the current density is set to the maximum of $21A_{rms}/mm^2$ for armature winding and $21A/mm^2$ for excitation coil. The outer diameter 264mm and the stack length 70mm of main part of the design machine are identical with those of IPMSM. It can be expected that the rotor structure is mechanically robust to rotate at high speed because it consists of only stacked soft iron sheets, so that the target maximum operating speed is elevated up to 20,000r/min. The target maximum torque 210Nm is determined from a realization of comparable maximum axle torque with the present IPMSM via reduction gear ratio of 4:1. The target maximum power is set to be more than 123kW and the motor weight to be designed is less than 35kg, resulting in that the proposed machine promises to achieve the maximum power density of 3.5kW/kg similar with the estimated of IPMSM in LEXUS RX400h. Commercial FEA package, JMAG-Studio ver.10.0, released by Japanese Research Institute is used as 2D-FEA solver for this design.

Design parameters and procedures

Initially, performances of the proposed design machine as in Fig. 1 are calculated. The maximum torque and maximum power obtained are 176.4Nm and 91.7kW, respectively, which is far from the target requirements. To satisfy the requirements, design free parameters D_1 to D_7 are defined in rotor and stator part as illustrated in Fig. 3. The first step is carried out by updating rotor parameters, D_1, D_2 and D_3 while keeping D_4 to D_7 constant. Since the torque increases with the increase in rotor radius, D_1 is treated and considered as the dominant parameter to improve the torque. The obtained torque characteristic versus D_1 is shown in Fig. 4. From the figure, the torque is maximized when the rotor radius is 97.2mm. Then, keeping D_1 at 97.2 mm, the rotor pole depth D_2 and the rotor pole width D_3

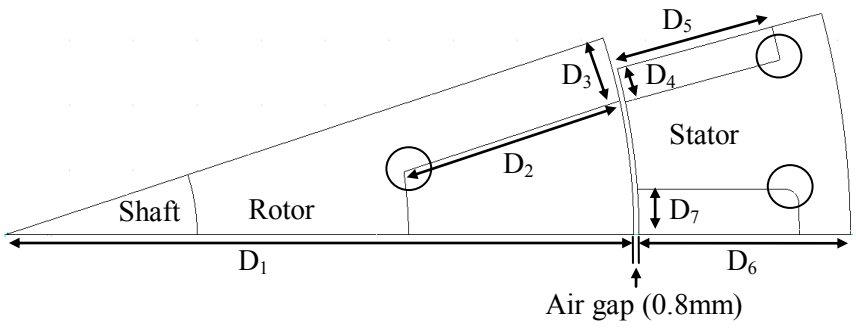

Fig. 3: Design parameters of 12Slot-10Pole FEFSSM

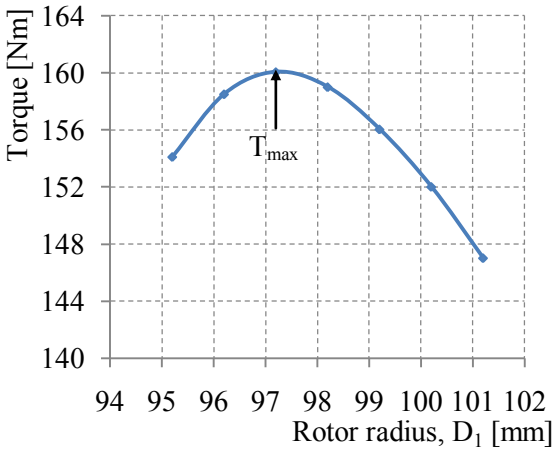

Fig. 4: Torque versus rotor radius D_1 characteristic

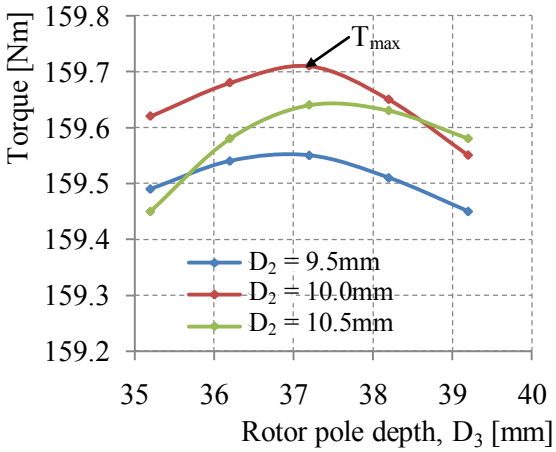

Fig. 5: Torque versus rotor pole depth D_3 for various rotor pole widths D_2

are adjusted. Fig. 5 illustrates the torque versus rotor pole depth D_2 for various rotor pole widths D_3. The torque is maximized when D_2 is 10.0mm and D_3 is 37.2mm. Once the maximum torque and power for D_2 and D_3 is determined, the second step is done by changing the excitation slot parameters D_4 and D_5 while keeping the rotor parameters and the slot area of armature winding S_a constant. Fig. 6 demonstrates the torque versus excitation coil width D_4 for various excitation coil height D_5. The maximum torque is obtained when D_4 is 10.0mm and D_5 is 20.0mm respectively. Then, using the maximum torque and power obtained from variation of D_4 and D_5, the armature slot area parameters D_6 and D_7 are treated with keeping other parameters discussed above constant. The necessary armature slot area S_a is determined by varying armature coil height, D_6 and armature coil width, D_7 to accommodate integer number of turns, N_a for armature coil. The plot of torque versus N_a is depicted in Fig. 7. The maximum torque and maximum power are obtained and well balanced when N_a is 7 turns, D_6 is 25.6mm and D_7 is 6.0mm, respectively.

The design methods explained above are treated repeatedly by changing D_1 to D_7 until the target torque and power are achieved. All design parameters are adjusted with keeping air gap length of 0.8mm constant under maximum current density condition. Finally, the corners circled in Fig. 3 are designed for the flux to flow smoothly. As a result, the target torque-power of 210Nm and 123kW are realized. The final design of this machine, which satisfies the target requirements, is shown in Fig. 8. The comparisons between initial and final design parameters are listed in Table II.

Table II: Initial and final design parameters of 12Slot-10Pole FEFSSM

Parameter	Details	Initial	Final
D_1	Rotor radius (mm)	96.2	98.2
D_2	Rotor pole depth (mm)	10.5	10.0
D_3	Rotor pole width (mm)	32.2	35.2
D_4	Permanent magnet length (mm)	7.2	7.8
D_5	Excitation coil pitch (mm)	20.0	23.1
D_6	Stator outer core thickness (mm)	25.6	23.6
D_7	Armature coil height (mm)	6.0	6.5
N_a	No. of turns of armature coil	7	7
AT_e	Excitation coil ampere turn (AT)	2330	2153
S_a	Armature coil area (mm^2)	152.7	152.7
S_e	Excitation coil area (mm^2)	194.2	179.4
T	Torque (Nm)	156.0	210.4
P	Power (kW)	106.8	123.0
pf	Power factor	0.56	0.64

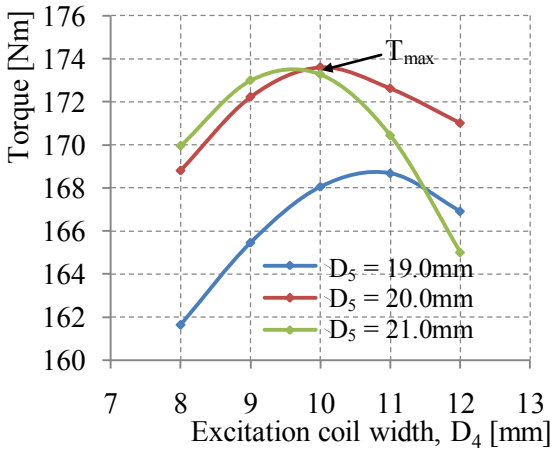

Fig. 6: Torque versus excitation coil width D_4 for different excitation coil height D_5

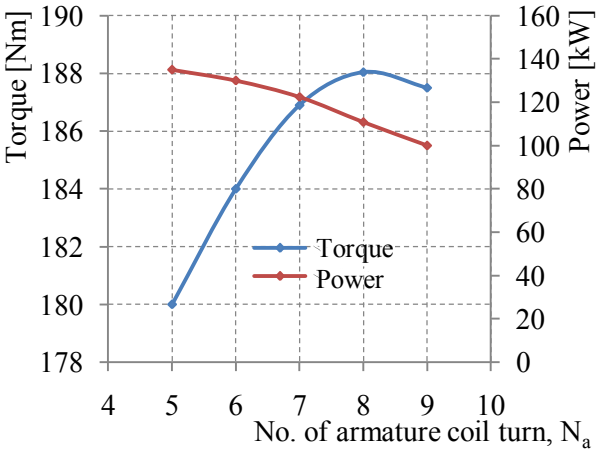

Fig. 7: Torque and power versus number of turns of armature winding N_a

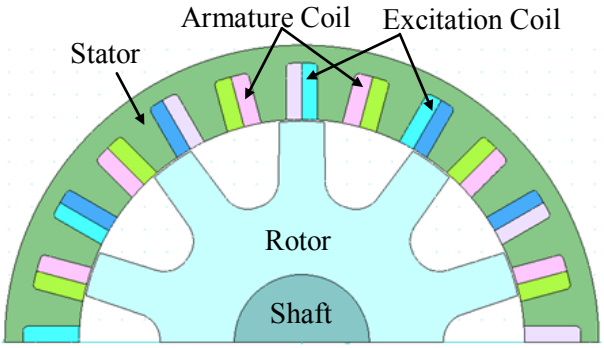

Fig. 8: Final design of 12Slot-10Pole FEFSSM (half model)

Results and performances

FEC flux linkage, emf and torque of the final designed machine

The open circuit field distribution for FEC are investigated based on FEA at maximum FEC current density. Basically, they are four typical rotor positions for the proposed machine as shown in Fig. 9. Obviously, the polarities of the phase FEC fluxes linked in the three phase armature coils are switched according to the rotor positions, realizing the "flux-switching". Meanwhile, Fig. 10 illustrates the emf waveforms of various FEC current densities, J_e at 3000r/min. The emf at low FEC current density is more sinusoidal compared with high FEC current density, while the FEC current densities higher than 15A/mm^2 show similar emf characteristics. Fig. 11 compares the target 210Nm torque waveforms obtained based on FEA and analytical at maximum current density of both FEC and armature coils. Clearly, good agreements are achieved and the peak-peak torque value is less than 6% of the maximum. At this condition, the target power reached 123kW when the speed is at 5584r/min.

Torque and power factor versus J_e characteristics

The torque and power factor versus FEC current density, J_e characteristics are plotted in Fig. 12 and Fig. 13, respectively, where both armature current density, J_a and FEC current density, J_e are varied from 0 to 21A/mm^2. From both figure, an increase in the armature current density will increase torque but reduce power factor. However, with the increase in FEC current density, the power factor can be improved and kept constant even if the armature current density is very high. The plots clearly show the target maximum torque is obtained when J_a and J_e are set to 21A/mm^2 as their maximum.

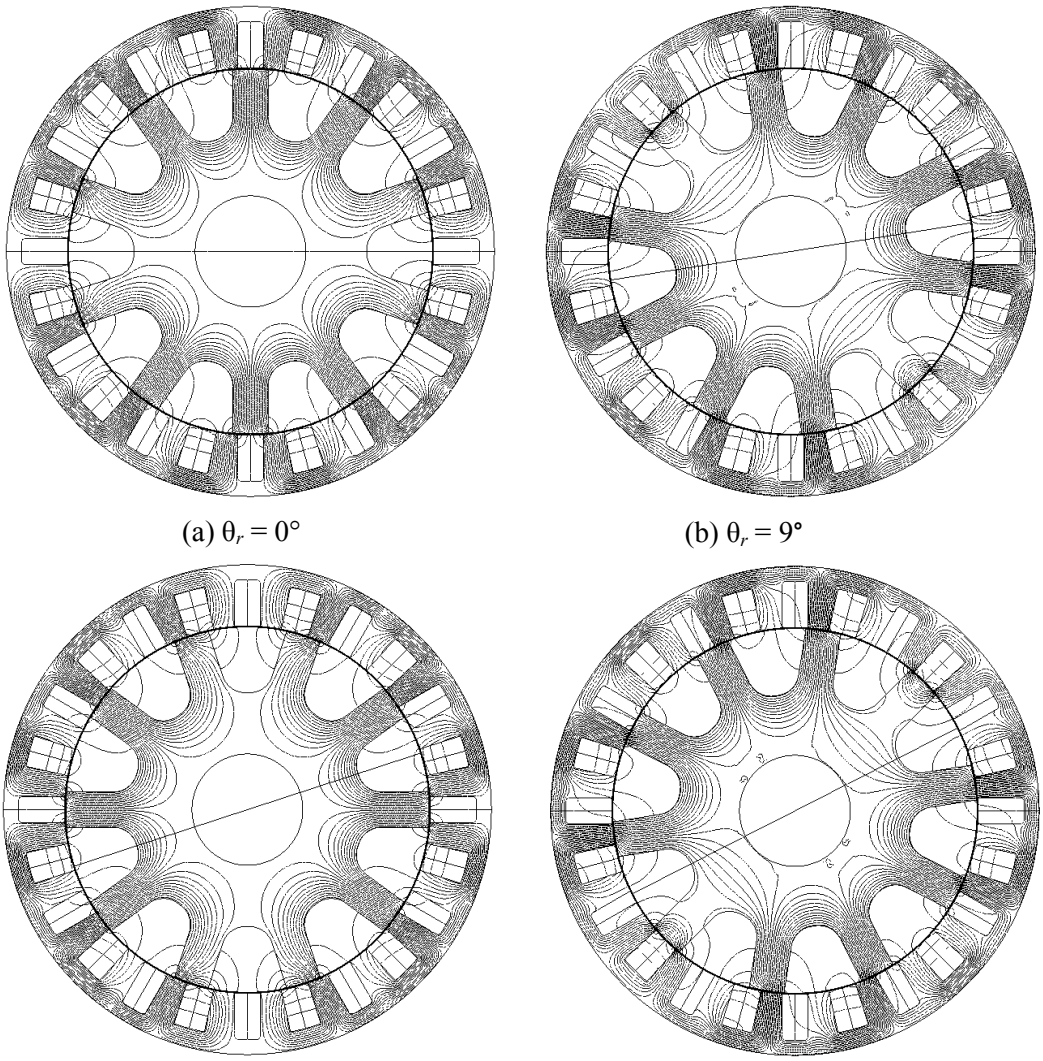

(a) $\theta_r = 0°$ (b) $\theta_r = 9°$

(c) $\theta_r = 18°$ (d) $\theta_r = 27°$

Fig. 9: Open circuit field distribution of FEC at four typical rotor positions, θ_r.

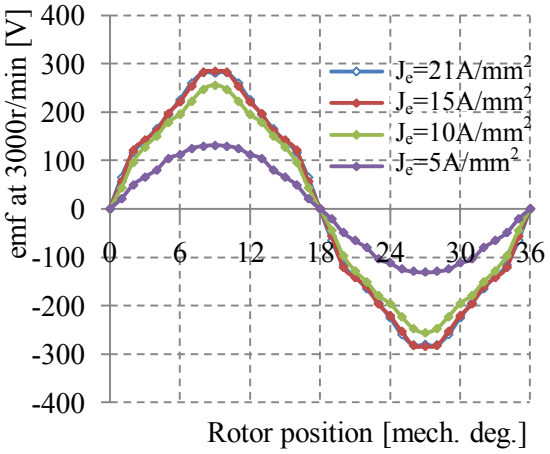

Fig. 10: Emf of various FEC at 3000r/min

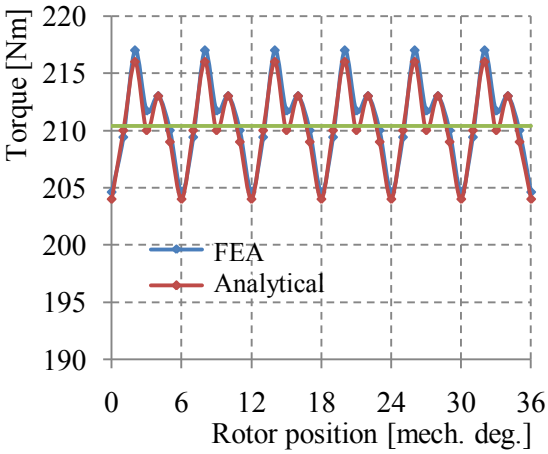

Fig. 11: Predicted torque waveforms based on FEA and analytical

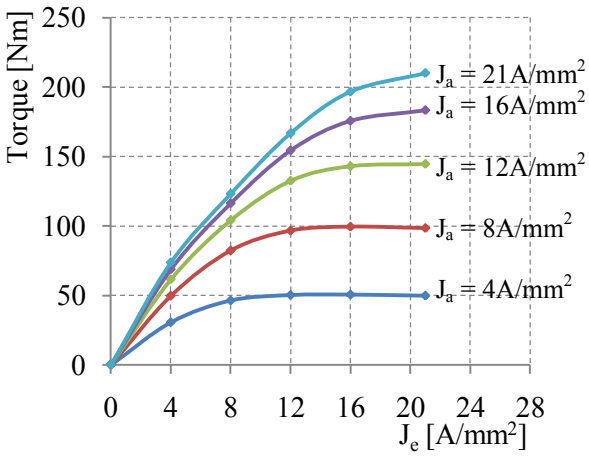

Fig. 12: Torque versus excitation current density, J_e at various armature current densities, J_a

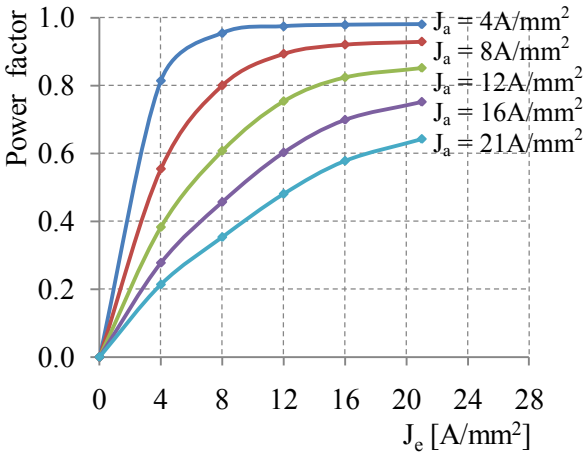

Fig. 13: Power factor versus excitation current density, J_e at various armature current densities, J_a

Torque and power versus speed characteristics

The torque and power versus speed curves of the designed motor is plotted in Fig. 14. At base speed 5,584r/min, the torque obtained is 210.4Nm as the maximum. The corresponding power reaches 123kW with power factor 0.644. The average power 131.7kW is achieved between 5,000 - 7,000r/min. The total weight of finally designed motor is 27.3kg and thus, the maximum torque density and power density are 7.7Nm/kg and 4.82kW/kg, respectively, which met the target requirement for HEV drive.

Motor loss and efficiency

The motor loss and efficiency are calculated by finite element analysis considering copper losses in the armature winding and iron losses in all laminated cores. Fig. 14 also demonstrates specific operating points at maximum torque, maximum power, and frequent operating point under light load driving condition noted as No. 1 to No. 8. Meanwhile, the detailed loss analysis and motor efficiency of this machine are illustrated in Fig. 15 where, P_o is the total output power, P_i is the iron loss and P_c is the copper loss. It can be expected that the designed machine realizes good efficiency at maximum torque (No. 1) and maximum power (No. 2). Furthermore, at frequent driving operation No. 3 to No. 8 under low load condition, the proposed machine achieves relatively high efficiency approximately more than 93%. At high speed operating point No. 2, the motor efficiency is degraded due to increase in iron loss, while at high torque operating points No.1, the efficiency is slightly degraded due to increase in copper loss. However, the proposed machine can still work at high efficiency as much as 92% to 95%.

Rotor mechanical stress at high speed

The mechanical stress prediction of the rotor structure at maximum speed 20,000r/min is executed by centrifugal force analysis based on 2D-FEA. The principal stress distributions of the rotor for the final designed motors are illustrated in Fig. 16. The maximum principal stress obtained is 92.2MPa which is much smaller than 300MPa being allowable as the maximum principal stress in conventional electromagnetic steel. This is a great advantage of FEFSSM with robust rotor structure that makes it more applicable to apply for high-speed HEV application compare to IPMSM.

Conclusion

In this paper, design optimization studies and performance analysis of a novel 12Slot-10Pole field-excitation flux switching synchronous machine (FEFSSM) for HEV application is presented. The goal of this research for an extension in speed and torque ranges is accomplished. The method of finding maximum performance of the machine is clearly demonstrated and met the target requirements. The proposed machine can keep the same power density as in existing IPMSM for LEXUS RX400h without any flux sources from permanent magnet.

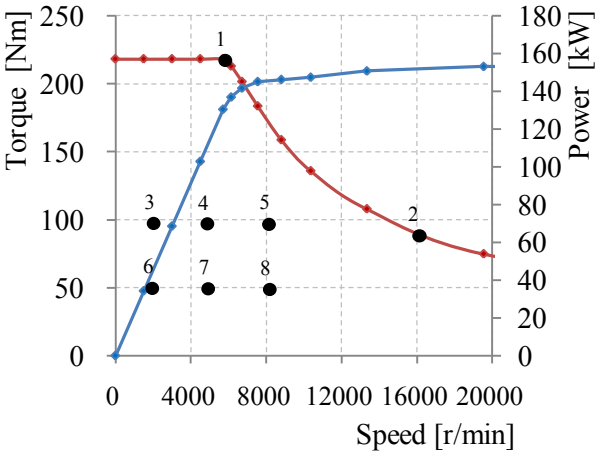

Fig. 14: Torque versus speed characteristics

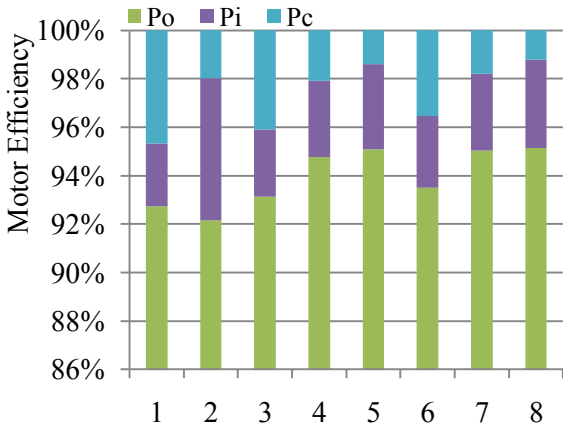

Fig. 15: Motor loss and efficiency

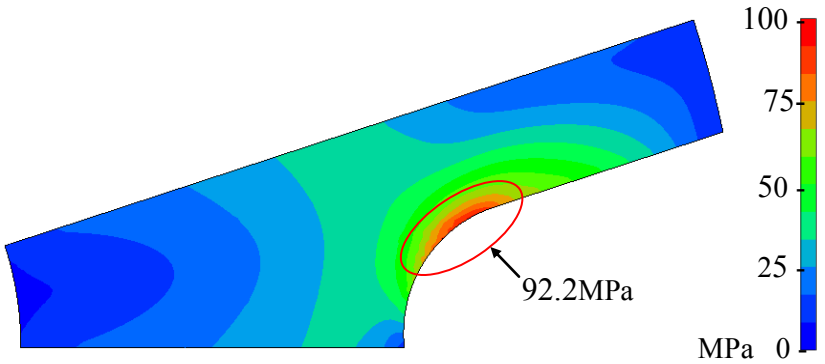

Fig. 16: Principal stress distributions of rotor at 20,000r/min

References

[1] C. Chan: "The state of the art of electric, hybrid, and fuel cell vehicles", *Proceedings IEEE*, vol. 95, no. 4, pp.704–718, April 2007.

[2] A. Emadi, J. L. Young, K. Rajashekara: "Power electronics and motor drives in electric, hybrid electric, and plug-in hybrid electric vehicles", *IEEE Transaction on Industrial Electronics*, vol.55, no.6, pp.2237-2245, Jan. 2008.

[3] M. Ehsani, Y. Gao, and J. M. Miller: "Hybrid electric vehicles: architecture and motor drives", *Proceedings IEEE*, vol. 95, no. 4, pp.719–728, April 2007.

[4] D. W. Gao, C. Mi, and A. Emadi: "Modeling and simulation of electric and hybrid vehicles", *Proceedings IEEE*, vol. 95, no. 4, pp.729–745, April 2007.

[5] T.Wang, P. Zheng, and S. Cheng: "Design characteristics of the induction motor used for hybrid electric vehicle", *IEEE Transaction on Magnetics*, vol. 41, no. 1, pp.505–508, Jan. 2005.

[6] X. D. Xue, K. W. E. Cheng, T. W. Ng, N. C. Cheung: "Multi-objective optimization design of in-wheel switched reluctance motors in electric vehicles", *IEEE Transaction on Industrial Electronics*, vol.57, no.9, pp.2980-2987, Sept. 2010.

[7] K. R. Geldhof, A. P. M. Van den Bossche, J. A. Melkebeek: "Rotor-position estimation of switched reluctance motors based on damped voltage resonance," *IEEE Transaction on Industrial Electronics*, vol.57, no.9, pp.2954-2960, Sept. 2010.

[8] S. M. Lukic, A. Emadi: "State-switching control technique for switched reluctance motor drives: Theory and implementation," *IEEE Transaction on Industrial Electronics*, vol.57, no.9, pp.2932-2938, Sept. 2010.

[9] K. T. Chau, C. C. Chan, and C. Liu: "Overview of permanent-magnet brushless drives for electric and hybrid electric vehicles", *IEEE Transaction on Industrial Electronics*, vol. 55, no.6 pp.2246–2257, June 2008.

[10] K. C. Kim, C. S. Jin, and J. Lee: "Magnetic shield design between interior permanent magnet synchronous motor and sensor for hybrid electric vehicle", *IEEE Transaction on Magnetics*, vol. 45, no.6 pp.2835–2838, June 2009.
[11] M. Kamiya: "Development of traction drive motors for the Toyota hybrid systems", *IEEJ Transaction on Industry Applications*, vol.126, no.4, pp.473-479, April 2006.
[12] R. Mizutani: "The present state and issues of the motor employed in Toyota HEVs", *Proc. of the 29th Symposium on Motor Technology in Techno-Frontier*, 2009, pp.E3-2-1-E3-2-20.
[13] Mineral Resource Information Center affiliated to Japan Oil, Gas and Metals National Corporation: "Metal resources report", vol. 36, no.1, 2006, pp.11-16.
[14] A. M. El-Refaie: "Fractional-slot concentrated-windings synchronous permanent magnet machines: Opportunities and challenges", *IEEE Transaction on Industrial Electronics*, vol.57, no.1, pp.107-121, Jan. 2010.
[15] T. Kosaka, T. Hirose and N. Matsui: "Brushless synchronous machine with wound-field excitation using SMC core designed for HEV drives", *Proc. The 2010 International Power Electronics Conference*, (IPEC 2010), Sapporo (Japan), June 2010.
[16] A. Zulu, B. C. Mecrow, and M. Armstrong: "A wound-field three-phase flux-switching synchronous motor with all excitation sources on the stator", *IEEE Transaction on Industry Applications*, vol. 46, no.6 pp.2363–2371, Nov. 2010.
[17] C. Pollock, et.al: "Flux-switching motors for automotive applications", *IEEE Transaction on Industry Applications*, vol. 42, no.5 pp.1177–1184, Sept. 2006.
[18] J. F. Bangura: "Design of high-power density and relatively high-efficiency flux-switching motor", *IEEE Transaction on Energy Conversion*, vol. 21, no.2 pp.416–425, June 2006.
[19] H. Wei, C. Ming, Z. Gan: "A novel hybrid excitation flux-switching motor for hybrid vehicles", *IEEE Transaction on Magnetics*, vol. 45, no.10 pp.4728–4731, Oct. 2009.